THz saturable absorption in turbostratic multilayer graphene on silicon carbide

Federica Bianco,[1,*] Vaidotas Miseikis,[2] Domenica Convertino,[2] Ji-Hua Xu,[1] Fabrizio Castellano,[1] Harvey E. Beere,[3] David A. Ritchie,[3] Miriam S. Vitiello,[1] Alessandro Tredicucci,[4] and Camilla Coletti[2]

[1]*NEST, Istituto Nanoscienze-CNR and Scuola Normale Superiore, P.za S. Silvestro 12, 56127 Pisa, Italy*
[2]*CNI@NEST, Istituto Italiano di Tecnologia, P.za S. Silvestro 12, 56127 Pisa, Italy*
[3]*Cavendish Laboratory, University of Cambridge, J. J. Thomson Avenue, Cambridge CB3 0HE, United Kingdom*
[4]*NEST, Istituto Nanoscienze-CNR and Dipartimento di Fisica "E. Fermi", Università di Pisa, L.go Pontecorvo 3, 56127 Pisa, Italy*
** federicabianco82@gmail.com*

Abstract: We investigated the room-temperature Terahertz (THz) response as saturable absorber of turbostratic multilayer graphene grown on the carbon-face of silicon carbide. By employing an open-aperture z-scan method and a 2.9 THz quantum cascade laser as source, a 10% enhancement of transparency is observed. The saturation intensity is several W/cm^2, mostly attributed to the Pauli blocking effect in the intrinsic graphene layers. A visible increase of the modulation depth as a function of the number of graphene sheets was recorded as consequence of the low nonsaturable losses. The latter in turn revealed that crystalline disorder is the main limitation to larger modulations, demonstrating that the THz nonlinear absorption properties of turbostratic graphene can be engineered via a proper control of the crystalline disorder and the layers number.

OCIS codes: (160.4236) Nanomaterials; (190.0190) Nonlinear optics; (190.4400) Nonlinear optics, materials; (140.5965) Semiconductor lasers, quantum cascade.

References and links

1. F. Bonaccorso, Z. Sun, T. Hasan, and A. C. Ferrari, "Graphene photonics and optoelectronics," Nat. Photonics **4**(9), 611–622 (2010).
2. A. Tredicucci and M. S. Vitiello, "Device Concepts for Graphene-based terahertz photonics," IEEE J. Sel. Top. Quantum Electron. **20**(1), 130–138 (2014).
3. V. Ryzhii, M. Ryzhii, and T. Otsuji, "Negative dynamic conductivity of graphene with optical pumping," J. Appl. Phys. **101**(8), 083114 (2007).
4. V. Ryzhii, A. A. Dubinov, T. Otsuji, V. Mitin, and M. S. Shur, "Terahertz lasers based on optically pumped multiple graphene structures with slotline and dielectric waveguides," J. Appl. Phys. **107**(5), 054505 (2010).
5. F. Rana, "Graphene terahertz plasmon oscillators," IEEE Trans. Nanotechnol. **7**(1), 91–99 (2008).
6. Y. Wu, D. B. Farmer, W. Zhu, S.-J. Han, C. D. Dimitrakopoulos, A. A. Bol, P. Avouris, and Y.-M. Lin, "Three-terminal graphene negative differential resistance devices," ACS Nano **6**(3), 2610–2616 (2012).
7. M. Breusing, C. Ropers, and T. Elsaesser, "Ultrafast carrier dynamics in graphite," Phys. Rev. Lett. **102**(8), 086809 (2009).
8. D. Sun, Z. K. Wu, C. Divin, X. Li, C. Berger, W. A. de Heer, P. N. First, and T. B. Norris, "Ultrafast relaxation of excited Dirac fermions in epitaxial graphene using optical differential transmission spectroscopy," Phys. Rev. Lett. **101**(15), 157402 (2008).
9. J. M. Dawlaty, S. Shivaraman, M. Chandrashekhar, F. Rana, and M. G. Spencer, "Measurement of ultrafast carrier dynamics in epitaxial graphene," Appl. Phys. Lett. **92**(4), 042116 (2008).
10. P. A. George, J. Strait, J. Dawlaty, S. Shivaraman, M. Chandrashekhar, F. Rana, and M. G. Spencer, "Ultrafast optical-pump terahertz-probe spectroscopy of the carrier relaxation and recombination dynamics in epitaxial graphene," Nano Lett. **8**(12), 4248–4251 (2008).
11. Q. Bao, H. Zhang, Y. Wang, Z. Ni, Y. Yan, Z. X. Shen, K. P. Loh, and D. Y. Tang, "Atomic-layer graphene as a saturable absorber for ultrafast pulsed lasers," Adv. Funct. Mater. **19**(19), 3077–3083 (2009).
12. S. Winnerl, F. Göttfert, M. Mittendorff, H. Schneider, M. Helm, T. Winzer, E. Malic, A. Knorr, M. Orlita, M. Potemski, M. Sprinkle, C. Berger, and W. A. de Heer, "Time-resolved spectroscopy on epitaxial graphene in the

#232493 - $15.00 USD Received 15 Jan 2015; revised 5 Apr 2015; accepted 9 Apr 2015; published 24 Apr 2015

infrared spectral range: relaxation dynamics and saturation behavior," J. Phys. Condens. Matter **25**(5), 054202 (2013).
13. R. Paiella, "Terahertz quantum cascade lasers: going ultrafast," Nat. Photonics **5**(5), 253–255 (2011).
14. C. Y. Wang, L. Diehl, A. Gordon, C. Jirauschek, F. X. Kärtner, A. Belyanin, D. Bour, S. Corzine, G. Höfler, M. Troccoli, J. Faist, and F. Capasso, "Coherent instabilities in a semiconductor laser with fast gain recovery," Phys. Rev. A **75**(3), 031802 (2007).
15. S. Barbieri, M. Ravaro, P. Gellie, G. Santarelli, C. Manquest, C. Sirtori, S. P. Khanna, E. H. Linfield, and A. G. Davies, "Coherent sampling of active mode-locked terahertz quantum cascade lasers and frequency synthesis," Nat. Photonics **5**(5), 306–313 (2011).
16. J. Maysonnave, K. Maussang, J. R. Freeman, N. Jukam, J. Madéo, P. Cavalié, R. Rungsawang, S. P. Khanna, E. H. Linfield, A. G. Davies, H. E. Beere, D. A. Ritchie, S. S. Dhillon, and J. Tignon, "Mode-locking of a terahertz laser by direct phase synchronization," Opt. Express **20**(19), 20855–20862 (2012).
17. M. C. Hoffmann and D. Turchinovich, "Semiconductor saturable absorbers for ultrafast terahertz signals," Appl. Phys. Lett. **96**(15), 151110 (2010).
18. M. C. Hoffmann, J. Hebling, H. Y. Hwang, K.-L. Yeh, and K. A. Nelson, "THz-pump/THz-probe spectroscopy of semiconductors at high field strengths (Invited)," J. Opt. Soc. Am. B **26**(9), A29–A34 (2009).
19. Z. Sun, T. Hasan, F. Torrisi, D. Popa, G. Privitera, F. Wang, F. Bonaccorso, D. M. Basko, and A. C. Ferrari, "Graphene mode-locked ultrafast laser," ACS Nano **4**(2), 803–810 (2010).
20. M. N. Cizmeciyan, J. W. Kim, S. Bae, B. H. Hong, F. Rotermund, and A. Sennaroglu, "Graphene mode-locked femtosecond Cr:ZnSe laser at 2500 nm," Opt. Lett. **38**(3), 341–343 (2013).
21. I. H. Baek, H. W. Lee, S. Bae, B. H. Hong, Y. H. Ahn, D. I. Yeom, and F. Rotermund, "Efficient mode-locking of sub-70-fs Ti:Sapphire laser by graphene saturable absorber," Appl. Phys. Express **5**(3), 032701 (2012).
22. Z. Zheng, C. Zhao, S. Lu, Y. Chen, Y. Li, H. Zhang, and S. Wen, "Microwave and optical saturable absorption in graphene," Opt. Express **20**(21), 23201–23214 (2012).
23. H. Y. Hwang, N. C. Brandt, H. Farhat, A. L. Hsu, J. Kong, and K. A. Nelson, "Nonlinear THz conductivity dynamics in p-type CVD-grown graphene," J. Phys. Chem. B **117**(49), 15819–15824 (2013).
24. W. S. Bao, S. Y. Liu, and X. L. Lei, "Hot-electron transport in graphene driven by intense terahertz fields," Phys. Lett. A **374**(10), 1266–1269 (2010).
25. W. S. Bao, S. Y. Liu, X. L. Lei, and C. M. Wang, "Nonlinear DC transport in graphene," J. Phys. Condens. Matter **21**(30), 305302 (2009).
26. P. Bowlan, E. Martinez-Moreno, K. Reimann, T. Elsaesser, and M. Woerner, "Ultrafast terahertz response of multilayer graphene in the nonperturbative regime," Phys. Rev. B **89**(4), 041408 (2014).
27. P. Bowlan, E. Martinez-Moreno, K. Reimann, M. Woerner, and T. Elsaesser, "Terahertz radiative coupling and damping in multilayer graphene," New J. Phys. **16**(1), 013027 (2014).
28. C. L. Frewin, C. Coletti, C. Riedl, U. Starke, and S. E. Saddow, "A Comprehensive study of hydrogen etching on the major SiC polytypes and crystal orientations," Mater. Sci. Forum **615–617**, 589–592 (2009).
29. M. Sprinkle, D. Siegel, Y. Hu, J. Hicks, A. Tejeda, A. Taleb-Ibrahimi, P. Le Fèvre, F. Bertran, S. Vizzini, H. Enriquez, S. Chiang, P. Soukiassian, C. Berger, W. A. de Heer, A. Lanzara, and E. H. Conrad, "First direct observation of a nearly ideal graphene band structure," Phys. Rev. Lett. **103**(22), 226803 (2009).
30. P. Mallet, F. Varchon, C. Naud, L. Magaud, C. Berger, and J.-Y. Veuillen, "Electron states of mono- and bilayer graphene on SiC probed by scanning-tunneling microscopy," Phys. Rev. B **76**(4), 041403 (2007).
31. C. Faugeras, A. Nerrière, M. Potemski, A. Mahmood, E. Dujardin, C. Berger, and W. A. de Heer, "Few layer graphene on SiC, pyrolitic graphite and graphene: a Raman scattering study," Appl. Phys. Lett. **92**(1), 011914 (2008).
32. A. C. Ferrari and D. M. Basko, "Raman spectroscopy as a versatile tool for studying the properties of graphene," Nat. Nanotechnol. **8**(4), 235–246 (2013).
33. L. G. Cançado, A. Jorio, E. H. Ferreira, F. Stavale, C. A. Achete, R. B. Capaz, M. V. O. Moutinho, A. Lombardo, T. S. Kulmala, and A. C. Ferrari, "Quantifying defects in graphene via Raman spectroscopy at different excitation energies," Nano Lett. **11**(8), 3190–3196 (2011).
34. H.-W. Hübers, S. Pavlov, A. Semenov, R. Köhler, L. Mahler, A. Tredicucci, H. Beere, D. Ritchie, and E. Linfield, "Terahertz quantum cascade laser as local oscillator in a heterodyne receiver," Opt. Express **13**(15), 5890–5896 (2005).
35. T. Hasan, Z. Sun, F. Wang, F. Bonaccorso, P. H. Tan, A. G. Rozhin, and A. C. Ferrari, "Nanotube–polymer composites for ultrafast photonics," Adv. Mater. **21**, 3874–3899 (2009).
36. H. Yang, X. Feng, Q. Wang, H. Huang, W. Chen, A. T. S. Wee, and W. Ji, "Giant two-photon absorption in bilayer graphene," Nano Lett. **11**(7), 2622–2627 (2011).

1. Introduction

The great interest graphene is attracting for THz optoelectronic and photonic applications [1] is well demonstrated by the numerous graphene-based devices recently proposed for the manipulation and detection of THz waves [2]. Furthermore, the unique properties of this peculiar 2D material make it highly promising even for the development of THz sources. For example, the possibility to achieve THz gain has been examined through interband population

#232493 - $15.00 USD Received 15 Jan 2015; revised 5 Apr 2015; accepted 9 Apr 2015; published 24 Apr 2015

inversion [3–5], as well as via the negative differential resistance (NDR) in the transport characteristics of an electronic device [6]. Interestingly, thanks to its fast carrier dynamics (on the picosecond time scale [7–10]) and the possibility to saturate the absorption in a broadband spectral range [11, 12] with relatively low-power incident radiation, graphene may also be a potential candidate for the generation of ultrashort THz pulses by means of passive mode-locking of already existing THz sources, such as Quantum Cascade Lasers (QCLs). In fact, owing to the strong electron-phonon interaction in the gain medium, the intersubband transitions of QCLs are characterized by a short relaxation time (of the order of tens of ps in the THz range and 1 ps in the mid-IR). This may complicate the achievement of passive mode locking [13, 14] with respect to the common ultrashort pulsed laser systems (where the gain recovery time is much longer). In fact, it poses stringent requirements on the saturable absorber dynamics, even when the conventional passive mode locking conditions are satisfied, i.e. when the gain recovery time is longer than cavity roundtrip time (64 ps for a 3 mm long cavity). Currently, mode locking in QCLs has been demonstrated via active techniques, employing either radiofrequency synthesizers for current modulation [15] or, indirectly, through a combined injection seeding and phase synchronization approach [16]. However, in both cases external cavity control is a mandatory constraint. It has to be mentioned that potential saturable absorbers for THz sources like p-Ge lasers or QCLs have been identified in n-type semiconductors (e.g. GaAs, Ge, GaP), where the absorption bleaching is based on the lowering of the electron conductivity at high momentum states (where the conduction band nonparabolicity is pronounced) and on the scattering into satellite valleys [17]. Nevertheless, such effect is achievable only under strong THz electric field, i.e. larger than tens of kV/cm [18]. As an alternative, graphene could offer a sufficiently short temporal response of the absorption saturation, as well as a potentially lower electric field strength requirement (depending on the driving bleaching mechanism, as it will be discussed in the following). Of course, the condition that the gain recovery time would exceed the cavity roundtrip one would still have to be satisfied by suitable active region design and resonator engineering.

The ultrafast broadband saturable absorption properties of graphene have been recently proven in a wide range of near- and mid-infrared wavelengths both in single- and multi-layer structures with successful integration in bulk and fiber lasers [11, 19–21]. Additionally, absorption bleaching has been reported in the microwave range [22], pointing out the lowering of the saturation intensity threshold for longer excitation wavelengths. Light-induced transparency has been observed in a single layer of highly doped graphene under intense ps-long THz pulses [23]. The nonlinear dependence of the intraband photoconductivity on the THz field strength [24,25] has been identified as the driving source of the saturable absorption properties; on the contrary, the Pauli blocking effect occurring in the interband transitions has been deemed unlikely in this type of samples. Moreover, the nonlinear THz response of multilayer epitaxial graphene has been studied in the excitation regime where the interaction of electrons with the external field dominates over the scattering processes [26,27]. In this regime the very intense electric field carried by the THz pulses leads to a coherent interplay of both inter- and intraband transitions, ultimately leading to an increase of the graphene absorption.

In this letter, we report on the experimental evidence of saturable absorption in undoped turbostratic multilayer graphene in a quasi-continuous (cw) THz excitation regime. The open-aperture z-scan method was applied to fully characterize the pump-intensity dependence of the graphene absorption. Light-induced transparency was observed with a few percent rise in the graphene transmission as a consequence of the absorption bleaching. The main mechanisms associated to the observed transmission enhancement were discussed with respect to the specific sample characteristics, i.e. hierarchical isolated-graphene-like behavior of the multilayer stack and doping effect, resulting in a dominant Pauli blocking regime despite the THz frequency of the radiation. Saturation intensity and modulation depth were

#232493 - $15.00 USD Received 15 Jan 2015; revised 5 Apr 2015; accepted 9 Apr 2015; published 24 Apr 2015

then studied as a function of the sample thickness, pointing out the possibility to tune the saturation properties through the number of graphene layers. Finally, the main limitations for a complete absorption saturation were analyzed through a careful study of the crystalline disorder of the graphene sheets.

2. Graphene fabrication and characterization

A set of three samples was investigated. The latters were graphene multilayers grown via chemical vapor deposition (CVD) on the carbon-terminated surface of an insulating silicon carbide substrate (4H-SiC (000 $\bar{1}$)) at a common pressure of 750 mbar. Prior to growth, the samples were hydrogen etched to remove polishing scratches and reveal atomic steps [28]. Both hydrogen etching and growth were performed in a resistively heated cold-wall reactor (high-temperature Aixtron BM). Temperature, growth time and gas flow of methane (CH_4) were 1410 °C, 3′ and 2 sccm for sample 1 and 1380 °C, 3′ and 10 sccm for sample 2. Sample 3 was grown by flowing 5 sccm of CH_4 first at 1320 °C for 1′ and then at 1340 °C for 4′. The argon (Ar) gas flow was 500 sccm in all cases. The number of layers was estimated from the flat absorption in the infrared region measured by Fourier transform infrared (FTIR) spectroscopy and it corresponds to approximately 25 layers for sample 1, 80 layers for sample 2 and 85 layers for sample 3. The multilayer epitaxial growth on the carbon-face ensured a very low unintentional doping only for the first few layers [29] and a negligible interaction of subsequent layers with the substrate [30].

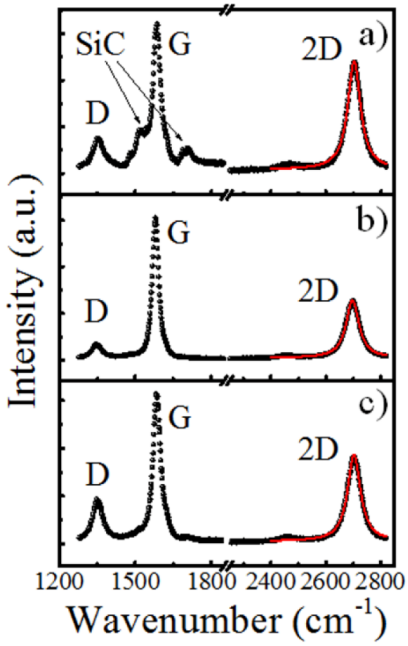

Fig. 1. Representative Raman spectra measured at a pumping wavelength of 532 nm for the sample 1 (a), 2 (b), 3 (c). The red solid lines are single Lorentzian fits.

Moreover, micro-Raman spectroscopy revealed the growth of loosely stacked layers, as demonstrated by the single Lorentzian shape of second order Raman band (2D peak) [31] (Fig. 1(a)-1(c)). Under these conditions, it is fair to assume that the optical properties of the samples arise from the superposition of the monolayer-like optical response of each layer. In all the samples the first order D peak at about 1350 cm^{-1} was also observed. Generally, in pristine graphene this band is forbidden by the scattering selection rules, as it is related to the breathing modes of the six-atom rings, and requires defects in the sheet to be Raman activated

#232493 - $15.00 USD Received 15 Jan 2015; revised 5 Apr 2015; accepted 9 Apr 2015; published 24 Apr 2015

[32]. Consequently, the D peak can be used to establish the quality of the graphene and in particular, the ratio of D and G peaks intensities (I_D/I_G) and full-width at half maximum (Γ_G) of the G peak quantify and discriminate the disorder within the graphene [9,32,33]. Considering I_D/I_G and Γ_G values from the Raman spectra of Fig. 1(a)-(c) measured at 532 nm, all samples have a relatively low disorder and are in the low-defect-density regime [33].

3. THz optical saturable absorption

The nonlinear properties of the samples were investigated at room temperature by collecting the light transmitted through the sample when it is translated along the optical axis around the beam focus, as typically done in the open-aperture z-scan technique. The laser beam of a 2.9 THz QCL, operated in a long-pulse regime (15% duty cycle, corresponding to 300 kHz frequency and 500 ns pulse width, further modulated at 4 Hz by a square function at 50% duty cycle), was focused onto the sample with a beam waist of about 170 μm. The data were collected at two different excitation peak intensities, i.e. about 130 and 220 mW/cm^2 (at the focal point), and the transmitted beam was detected by a thin film-based single element thermopile detector (2M from Dexter).

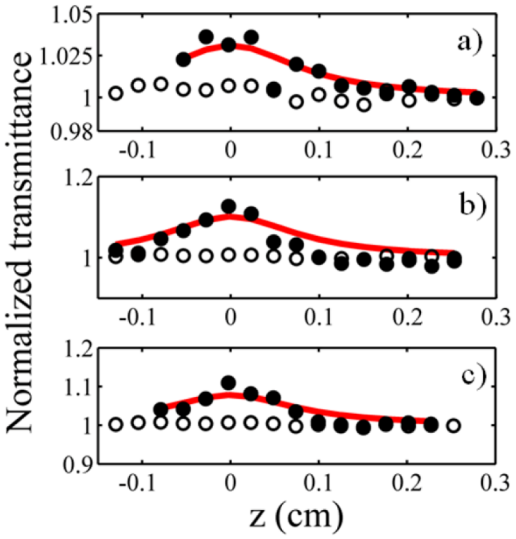

Fig. 2. Z-scan traces of the sample 1 (a), 2 (b), 3 (c) (solid dots) and of the substrate (empty dots). The red lines are the fit curves assuming the simple two-level saturable absorber model.

Figures 2(a)-2(c) show the z-scan traces normalized with respect to the substrate linear transmission when an excitation intensity of about 220 mW/cm^2 was used. The typical signature of the absorption bleaching was observed at the focal point z = 0, where the z-scan trace manifests a maximum. This corresponds to a sample transmission enhancement of about 4% in sample 1 and 10% in samples 2 and 3. No similar feature was found in the substrate transmission at the same input intensity scale (empty dots in Figs. 2(a)-2(c)).

In order to analyze the absorption properties, the simple two-level saturable absorber model was assumed. Therefore, taking into account the nearly circular Gaussian spatial profile [34] and the quasi-continuous wave driving regime of the QCL (so that the beam intensity is assumed time-independent), the dependence of the absorption coefficient on the pump intensity is expressed as:

$$\alpha(I) = \alpha_{NS} + \frac{\alpha_S}{1 + \frac{I_0(z)}{I_S}} \quad (1)$$

#232493 - $15.00 USD Received 15 Jan 2015; revised 5 Apr 2015; accepted 9 Apr 2015; published 24 Apr 2015

where α_{NS} and α_S are the nonsaturable and saturable components of the linear absorption α_0 (where $\alpha_0 = \alpha(I_0 \rightarrow 0)$), respectively. $I_0(z)$ is the beam intensity along the optical axis (where $I_0(z) = I_0/(1 + (z/z_R)^2)$, with I_0 being the time-independent on-axis intensity and z_R the Rayleigh range), while Is is the saturation intensity, i.e. the intensity at which the saturable absorption is reduced to 1/2.

The fit of z-scan data, assuming I_s and α_s as free parameters and taking into account the measured samples reflectivity, reveals that the saturation intensity increases with the number of layers (Fig. 3(a)), ranging from 4 ± 1 W/cm^2 in sample 1 to 10 ± 1 W/cm^2 in sample 3, corresponding to a saturation fluence of several μJ/cm^2.

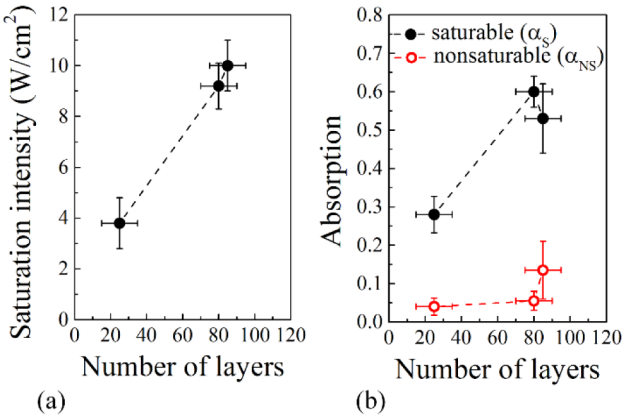

Fig. 3. (a) Saturation intensity as a function of the layers number. (b) Saturable (black solid circles) and nonsaturable (red empty circles) absorption coefficients as a function of the layers number. The dashed lines are guides to the eye.

Two mechanisms can be identified as the main causes of the observed absorption bleaching in our samples. The predominant one we believe originates from the Pauli blocking effect. Thanks to the mostly intrinsic nature of the isolated graphene layers, the overall optical properties can indeed be assumed to be driven by interband excitation even in the THz region, as confirmed by the nearly flat spectral dependence of the THz transmission observed with FTIR spectroscopy (Fig. 4), as well as by magneto-optics measurements that quantified the Fermi level to be lower than 10 meV.

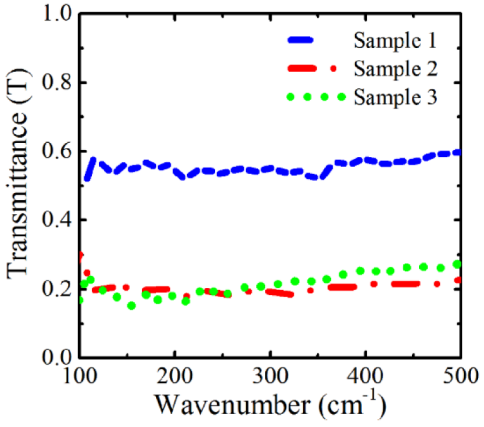

Fig. 4. Transmittance spectrum in the THz region for sample 1 (blue dashed line), sample 2 (red dashed-dotted line) and sample 3 (green dotted line).

#232493 - $15.00 USD Received 15 Jan 2015; revised 5 Apr 2015; accepted 9 Apr 2015; published 24 Apr 2015

This implies that the larger the number of layers, the more intense the THz excitation is needed to generate the proper concentration of photogenerated carriers able to prevent further absorption of photons. It is worth noting that the saturation intensity resulted four orders of magnitude lower than those observed in the near infrared [11]. This is not unexpected as the Dirac-like dispersion relation for both electrons and holes, preserved in our samples by the decoupling of layers, possesses a much lower density of states at long wavelengths. This yields an easier band-state filling near the Dirac point, thus requiring lower radiation intensity to reach Pauli blocking conditions. Secondly, a minor contribution from the first lightly doped layers, where intraband transitions are dominant, cannot be ruled out. In this case, the absorption bleaching is expected to arise from the lowering of the optical conductivity under intense THz electric field due to the induced faster carrier dynamics with the consequent suppression of the carrier mobility [23–25]. One has to notice that, in the present experiment, the electric field carried by the quasi continuous wave THz source is about 10 V/cm, thus coherently driven dynamics [26, 27] may be excluded, since such contributions have been observed with THz electric fields of the order of kV/cm.

All of the samples exhibited good nonlinear absorption properties (Fig. 3(b)). The maximum value of modulation depth (α_S) was estimated as high as 60 ± 4% in sample 2, while all of the samples were characterized by a quite low nonsaturable absorption (α_{NS} < 15%). As shown in Fig. 3(b), the ultimate gain in the transparency to THz waves is strongly determined by the thickness of the sample. Specifically, it was found that the thicker the sample, the higher the modulation depth. Remarkably, this behavior may ensure a possible fine tuning of α_S only by means of the sample thickness, as in a nearly ideal case. As a matter of fact, in real samples the capability to saturate the absorption is generally limited by the quality and by the specific characteristics of the sample and is quantified in terms of the nonsaturable component α_{NS}. Typically, nonsaturable losses originate from scattering losses at the interface between the layers [11], free carrier absorption or defect contributions [35]. While the latest depends on the quality of the fabrication technique, the other contributions may dominate under specific experimental conditions. Indeed, when short wavelengths are used, the dominant source is represented by the scattering losses at the layer interfaces [11], which is unavoidable even in case of defect-free graphene. On the contrary, for THz excitation, due to the long wavelength, the multi-interface effect has a minor contribution. Instead, when graphene is doped, the possible sources of nonsaturable absorption may remain linked to the free carrier absorption or to the reflectivity from the sheets, since in this regime the optical conductivity is well described by the Drude model. Finally, in both wavelength ranges nonlinear absorptive interactions, such as two photon absorption, may have to be taken into account under very intense illumination, since they mitigate the absorption saturation [36]. In the present case, due to the dominant interband optical conductivity and the relatively low pump intensity, the main limitation to the absorption saturation in our samples can be ascribed to the defects.

Although here all samples are in the limit of low defect density, the two-dimensional micro-Raman mapping revealed different degrees of disorder. Figure 5(a) reports the extremes of the interval of I_D/I_G values estimated in each sample.

#232493 - $15.00 USD Received 15 Jan 2015; revised 5 Apr 2015; accepted 9 Apr 2015; published 24 Apr 2015

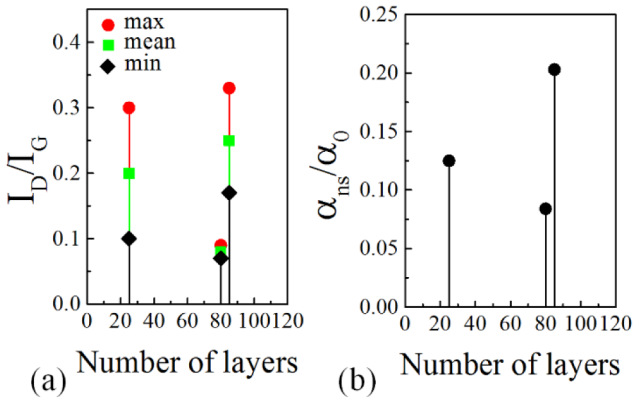

Fig. 5. (a) I_D/I_G as a function of the numbers of layers. Max (red circle), mean (green square) and min (black diamond) correspond to the maximum, mean and minimum values of I_D/I_G, respectively, as estimated from a representative micro-Raman mapped area (30x30 μm^2). (b) Ratio between the nonsaturable and the linear absorption coefficients as a function of the number of layers.

Sample 2 has good quality and homogeneity, with I_D/I_G ranging between 0.07 and 0.09, whereas samples 1 and 3 manifested slightly higher disorder and inhomogeneity ($I_D/I_G = 0.1 \div 0.3$ and $0.17 \div 0.33$, respectively). Ultrafast studies in similar samples [9,10] demonstrated a strong influence of defects on the graphene carrier dynamics. Particularly, it was shown that the slower relaxation time of the photogenerated carriers, which was related to the carrier-phonon scattering and possibly to electron-hole recombination, is inversely proportional to I_D/I_G [9]. From the comparison of Figs. 5(a) and 5(b), the contribution of nonsaturable absorption (expressed as α_{NS}/α_0 in Fig. 5(b) to define a parameter independent on the number of layers) is qualitatively well described by the crystallinity degree of the graphene (it is worth mentioning that the disorder contribution was actually averaged over the area probed by the spot size of the THz laser). Based on this result, α_{NS} in our samples may be explained as mainly arising from the defect-induced increased rate of the scattering processes, which is responsible for faster recovery times.

4. Conclusion

Open-aperture z-scan experiments were carried out to characterize the saturable absorption of multilayer turbostratic graphene in a long-pulse regime at 2.9 THz. Thanks to intrinsic nature of the multilayers, the Pauli blocking effect was identified as the dominant mechanism driving the absorption bleaching. The saturation intensity was estimated to be several W/cm^2. With respect to the linear absorption all samples showed large modulation depth, which was found increasing with the sample thickness, like in the nearly ideal case. From the analysis of the possible causes limiting the light-induced transparency in our samples, the absorption saturation resulted to be mainly influenced by the quality of the graphene sheets. As a consequence, for a specific number of layers, the maximum light-induced transparency in undoped turbostratic multilayer graphene is to be achieved predominantly through the control of the crystal disorder. This material represents a favorable platform for obtaining high performance THz saturable absorbers, which would pave the way to novel graphene-based mode-locked THz lasers.

Acknowledgments

The work was supported in part by the European Union Seventh Framework Programme under grant agreement n° 604391 Graphene Flagship.

#232493 - $15.00 USD Received 15 Jan 2015; revised 5 Apr 2015; accepted 9 Apr 2015; published 24 Apr 2015

MSV acknowledges financial support of the Italian Ministry of Education, University, and Research (MIUR) through the program “FIRB-Futuro in Ricerca 2010” RBFR10LULP “Fundamental research on Terahertz photonic devices”.

#232493 - $15.00 USD Received 15 Jan 2015; revised 5 Apr 2015; accepted 9 Apr 2015; published 24 Apr 2015